11-1-1994

Driven Front and Interface of a Fluid-Flow Model in 2+1-Dimensions

Michael J. Leaseburg
Louisiana State University

Ras B. Pandey
University of Southern Mississippi, ras.pandey@usm.edu

Driven front and interface of a fluid-flow model in 2+1 dimensions

Michael J. Leaseburg
Department of Physics and Astronomy, Louisiana State University, Baton Rouge, Louisiana 70803-4001

R. B. Pandey
Department of Physics and Astronomy, University of Southern Mississippi, Hattiesburg, Mississippi 39406-5046
(Received 28 February 1994)

Computer simulations are performed to study the motion of the front and the growth of the interface width in a model of fluid flow driven by a biased field in 2+1 dimensions. The initial motion of the front is diffusive, which is followed by a nondiffusive power-law behavior in the long-time regime; the power-law exponent is nonuniversal, varying with the strength of the driven field. The growth of the interface width saturates in the asymptotic time regime. The saturated width W scales with both the driven field B as well as the transverse length L of the sample, leading to a two-parameter scaling $W \sim L^{2\alpha} B^m$, where $\alpha = 1.25$ and $m = 0.17$.

PACS number(s): 68.10.Jy, 73.40.−c, 47.70.−n

For several years now [1–14], the study of interfacial dynamics and roughness growth has attracted continued interest, with efforts directed mostly toward the deposition models. Kinetics of the roughness growth in deposition models [4,5], and the dynamics of fronts in fluid-flow models [10–14], and the resulting interface, have some common features such as a similar power-law growth, and saturation of the interface width and its scaling with the size of the sample. Both the deposition models as well as the analysis of the fluid flow are motivated by their applications in understanding a variety of issues in diverse systems [5,15–17] such as growth of materials, mixing and phase separation in fluid, and wetting by imbibition. Fluid-flow models are particularly useful in understanding the front propagation in systems such as viscous fingering [18], imbibition [15], transport in porous media [19], and chemical reaction in additive polymerization [20], that are relatively easier to encounter in laboratories. A more specific application of our interest in fluid flow is to understand the spreading of the water from a source of a planar river front into the dry ground. Using a microscopic simulation, we attempt to address issues such as how fast the water front moves into the dry land, how much wet-land area is covered due to a specific mechanism (used here) for the frontal movement, and how it depends on the size of the source. Although a quantitative comparison of our results with such macroscopic fluid flow may not be feasible, prediction of the power laws for the qualitative behavior of the flow and spreading in simple model systems is possible, as we demonstrate in this paper. Furthermore, the general application of microscopic simulations to complex hydrodynamic phenomena, and complementary approaches to macroscopic hydrodynamic methods, has just begun [21,22], and we present some results using this approach.

A few preliminary studies have recently been reported about understanding the growth of fronts and the interface width in a few fluid-flow models which are limited to two dimensions [12–14]. While the stochastic mechanism of the mobile front and evolving interface show interesting power-law behaviors [12,13], the effect of the driven bias on these properties is relatively less understood. Because of major computational limitations, most of these studies [12–14] are devoted mainly to short-time behaviors i.e., to the temporal evolution of the interface growth. We present, a computer simulation study of the fluid-flow model in three dimensions, with the long-time regime extending far beyond the temporal evolution of the interface where the saturated interface width shows a scaling with both the size and the driven field.

We consider a three-dimensional discrete lattice of size $L_x \times L_y \times L_z$. The first yz plane (the base of the lattice) serves as a source of the wetting fluid which is spread into the lattice along the x direction by mobile particles. In the plane adjacent to the base, we randomly distribute a fixed number of particles (the carriers) N_p, which are initially wet and remain so for the duration of the simulation. Note that N_p may vary from 1 to $L_y \times L_z$, although we use the large value here in order to improve our statistics. After the initialization, the particles undergo stochastic motion in a biased field according to the following hopping probabilities. Motion in the $\pm y$ or $\pm z$ directions has the probabilities $P_{\pm y} = P_{\pm z} = \frac{1}{6}$, and along the x axis we have $P_{\pm x} = (1 \pm B_x)/6$, where $B_x \in [0,1]$ is the bias factor of the driven field. Thus the bias B_x drives the system of particles away from the source along the $+x$ direction, with no bias along the y or z axes. Our model is thus better deemed 2+1 dimensional.

Movement of the mobile particles is implemented by the following procedure. We randomly select a particle at a site i and one of its nearest neighbor sites, say j, in accordance with our hopping probabilities. If site j is empty, the particle relocates to site j, which then becomes permanently wet, an irreversible wetting; a site remains dry until it is visited by a particle. Periodic

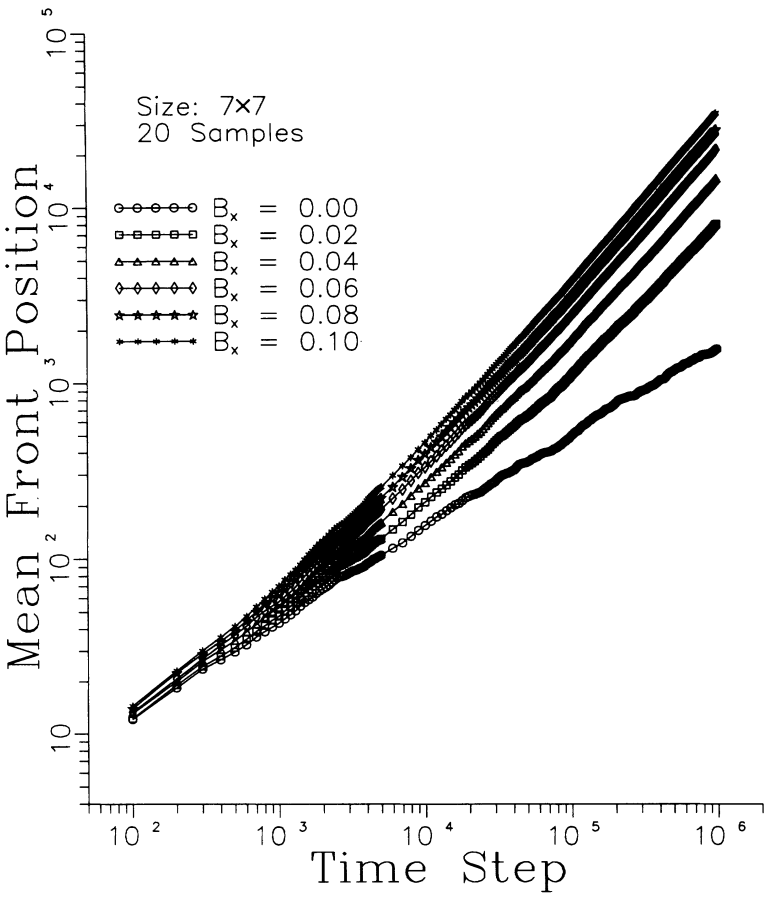

FIG. 1. Mean front position R_f vs (Monte Carlo) time steps (MCTS) for various values of B_x on a log-log scale.

boundary conditions are employed along the y and z axes and a reflecting boundary condition is in effect at the base. L_x is chosen so large that no particle traverses the entire lattice along the x direction during the course of the simulation (typically $L_x = 100\,000$). An attempt to move N_p particles once is defined as one time step. In order to obtain accurate averages we would ideally repeat this process for a large number of samples. Unfortunately, the long-time study with a large lattice results in an excessive execution time and, therefore, a large sampling is not feasible. We used 20 samples, each with a million time steps, and the simulations were carried out on RISC computer workstations.

At a time step we define the wetting front to be the locus of furthest wet sites along the x direction, i.e.,

$$R_f(t)=\frac{1}{L^2}\sum_{j,k}X_{jk}(t)\ , \tag{1}$$

where $X_{jk}(t)$ is the furthest x coordinate of the wet site (x,j,k). Thus the mean wetting front (R_f) is the average of the ensemble of wet sites. Notice that this definition, while standard, does not take into account the possibility of islands of dry sites. Also measured within each sample are the interface width (W), the average rms displacement of each particle ($R_{\rm tr}$), and that of their center of mass ($R_{\rm c.m.}$), which are defined as,

$$W^2(t)=\frac{1}{L^2}\sum_{jk}X_{jk}^2(t)-R_f^2(t)\ , \tag{2}$$

$$R_{\rm tr}^2(t)=\frac{1}{N_p}\sum_{i=1}^{N_p}[X_i^2(t)+Y_i^2(t)+Z_i^2(t)]\ , \tag{3}$$

$$R_{\rm c.m.}^2(t)=X_{\rm c.m.}^2(t)+Y_{\rm c.m.}^2(t)+Z_{\rm c.m.}^2(t)\ , \tag{4}$$

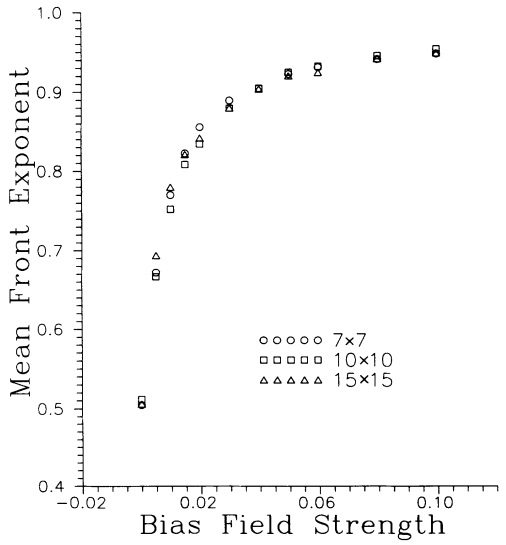

FIG. 2. The mean front exponent k of the power law $R_f \sim t^k$ vs B_x for samples $7\times7\times L_x$, $10\times10\times L_x$, and $15\times15\times L_x$, with $L_x = 100\,000$. 20 independent samples were used.

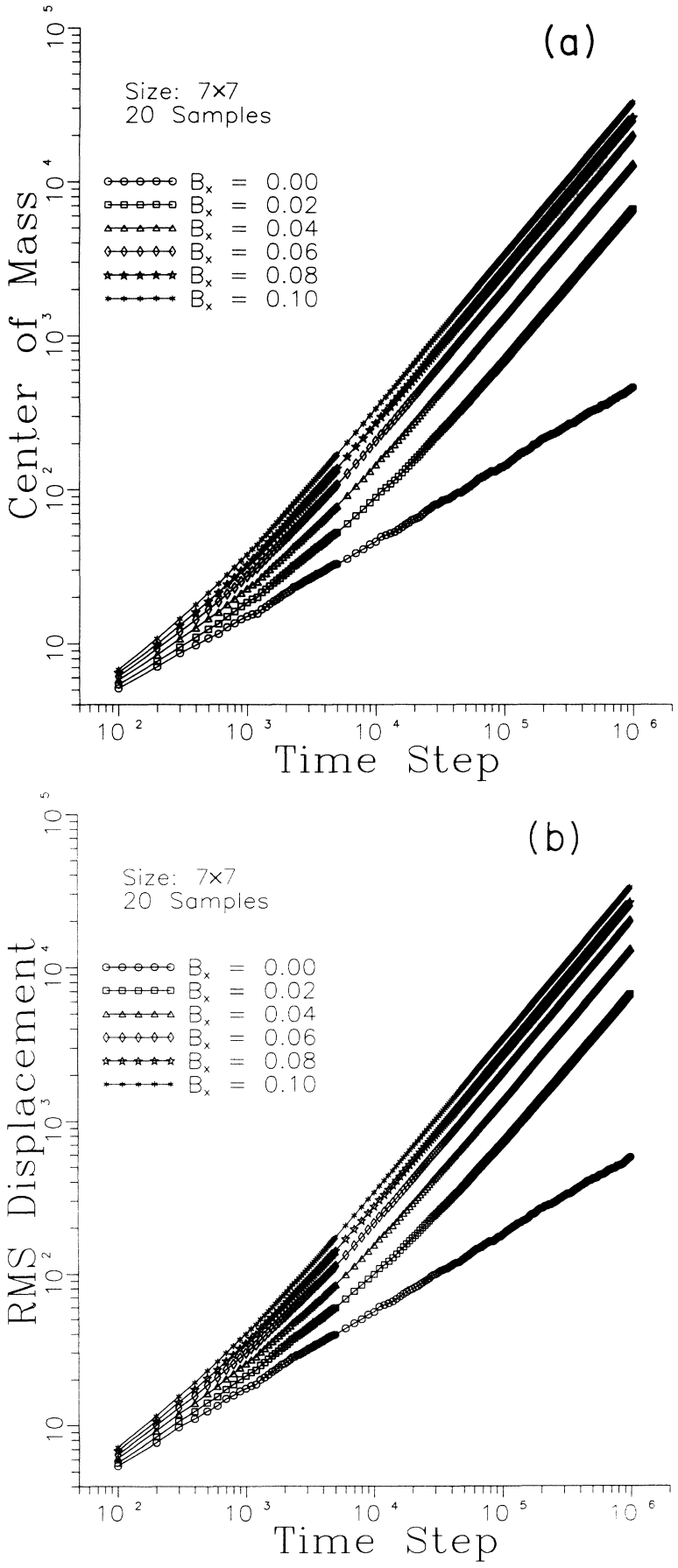

FIG. 3. Center of mass ($R_{\text{c.m.}}$) (a) and the rms displacement of particle (R_{tr}) (b) vs time step on a log-log scale.

$$X_{\text{c.m.}}=\frac{1}{N_p}\sum_{i=1}^{N_p}X_i\ ,\quad Y_{\text{c.m.}}=\frac{1}{N_p}\sum_{i=1}^{N_p}\ ,$$
$$Z_{\text{c.m.}}=\frac{1}{N_p}\sum_{i=1}^{N_p}Z_i\ , \tag{5}$$

where X_i, Y_i, and Z_i are the coordinates of the particle i. These four observables are then averaged again over the number of samples. We choose $L_y=L_z=L$ and samples with base sizes ($L_y\times L_z$) 7×7, 10×10, and 15×15 were used with values of L_x as large as 100 000. Data obtained become less noisy as the lattice size is increased. However, we present results for the smallest lattice where finite size effects should be most noticeable.

Figure 1 shows a plot of the mean wetting front R_f versus time for a range of B_x on a log-log scale. When $B_x=0.0$, the power law $R_f\sim t^k$ should exhibit a diffusive behavior ($k=\frac{1}{2}$), and we found an average exponent $k\simeq0.51\pm0.01$ for our three lattice sizes. As the biased field is increased, we find a much different behavior. In the short-time regime, the mean front shows the same power-law behavior for all nonzero values of B_x, while in the long-time regime the evolution of the wetting fronts obeys different power-law relations. The relaxation time for the crossover from short to long time (i.e., from similar to dissimilar) power-law behavior depends on the base size and the bias field strength. We estimate the magnitude of the asymptotic exponent k for various fields, and Fig. 2 shows a k versus B_x plot. At $B_x=0.0$, we observe a diffusive behavior, with $k\simeq0.5$, as previously mentioned. On increasing the magnitude of B_x, k increases with the field rather quickly at low biased regime. At higher values of B_x, however, the rate of increase slows down considerably. This variation of the exponent k with the field suggests that the asymptotic power-law motion of the front is nonuniversal. We should mention that the value of k appears to increase exponentially with respect to B_x, but this fit is difficult to predict more accurately due to the small range over which B_x varies.

Variation of the center of mass (c.m.) of the particles [Eqs. (4) and (5)] and their rms displacement [Eq. (3)] with time is presented in Figs. 3(a) and 3(b), respectively. With $B_x=0.0$ we find that the c.m. always trails the rms displacement of each particle, and this is a product of the diffusive nature of our system. However, for nonzero B_x

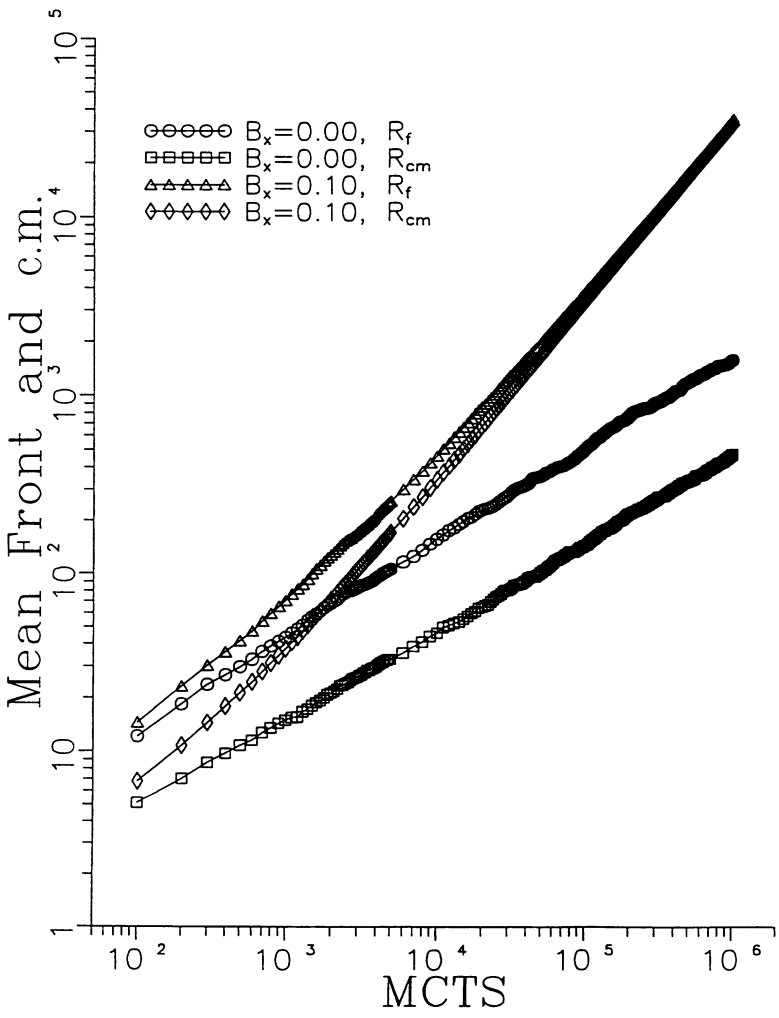

FIG. 4. Mean front and c.m. positions vs MCST time for $B_x=0.00$ and 0.10 on a log-log scale.

the differences become negligible as the system evolves. Looking at the trends in the motion of the c.m. and wetting front, we note that the c.m. lags behind the wetting front (see Fig. 4). Also evident in the nondiffusive evolutions is the speed with which the c.m. attempts to catch up with the front, and the approach to a saturation state for larger times. This behavior becomes more noticeable, as it should, upon increasing the strength of the bias field. Let us now examine the ratio $R_f/R_{\text{c.m.}}$, which is proportional to time as t^{k-l}. In case of diffusive behavior with $B_x=0.00$, we find the exponent $(k-l)$ ranging from 0.008 to 0.015 with an average value of 0.012 for our base sizes. This suggests that the ratio goes to infinity, as time tends toward infinity very slowly. For $B_x\neq 0.00$, however, we find $k-l$ to be negative, and $k-l$ decreases faster with increasing B_x, i.e., at $B_x=0.02$ the average value for $k-l$ is -0.139 and at $B_x=0.10$ it is -0.045. If we view an increase in the bias field as a method for rescaling time, these results suggest that the limiting value for $k-l$ is zero, and this approach to zero occurs slowly with respect to B_x (and thus in time). If this is indeed true we then have $R_f/R_{\text{c.m.}}\sim 1$. In the presence of a bias field such a ratio is expected because the c.m. should ride along the wetting front for large times.

Lastly, we studied the growth of the interface width W which is defined by $W^2=\langle R_f^2\rangle-\langle R_f\rangle^2$ [see Eq. (2) above]. Figure 5 is a plot of W versus time for various values of B_x and two lattice sizes. We immediately note that the finite size effects are transparent in the long-time regime, when the interface width saturates. In order to reach such an asymptotic (long-time) limit we have to resort to a small number of samples, which makes our analysis difficult due to large fluctuations. Nevertheless, it is evident, at least qualitatively, that the saturated width depends on both the size as well as the bias field strength.

We define the saturation width (W_s) as the average interface width over a long period of time after the saturation has been achieved. Both the onset time for saturation and the value for W_s appear to depend upon the base size and the bias field strength. The former result is best seen in the data for a sample size of 15×15. The W_s versus B_x plot is presented in Fig. 6. This figure shows a very nice linear relationship between these two quantities, and demonstrates an obvious size dependence. The increase in W_s with B_x is not surprising, however. Larger field strengths drive the particles to traverse the lattice more rapidly, resulting in larger fluctuations of the wetting front. Even with large error bars in the average estimates of the saturated widths, its dependence on the field strength and the base size is relatively easier to evaluate. This led us to consider the possibility of a scaling behavior. It is rather difficult to devise a two-parameter scaling for the saturated width. However, since W_s varies with B_x and base size, it is natural to examine our results as a scaling $W_s\sim A^{\alpha}f(B_x)$, where $A=L_y\times L_z$

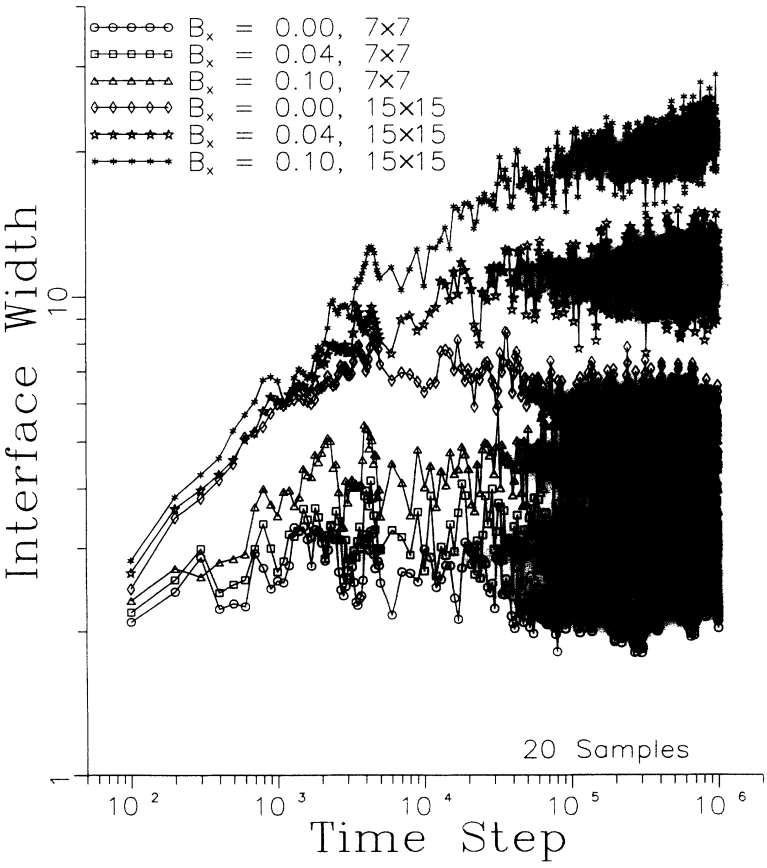

FIG. 5. Interface width vs time step on a log-log scale for various values of B_x with samples $7\times 7\times L_x$ and $15\times 15\times L_x$; $L_x=100\,000$.

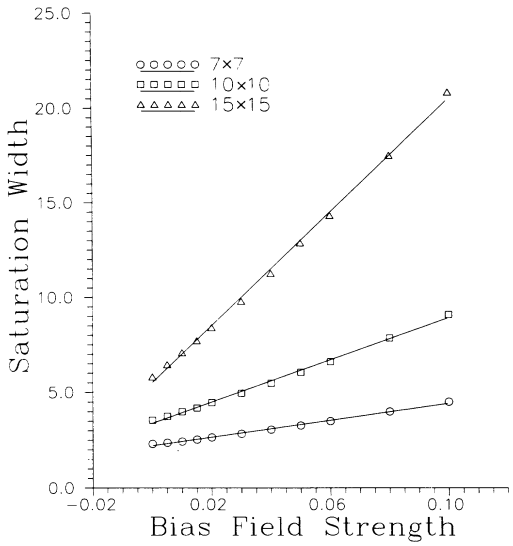

FIG. 6. Saturated width W_s vs B_x for three base sizes (same statistics as Fig. 2). The last data points at the biased field strength 0.1 for each sample are 4.5 ± 0.6 (7×7), 9.1 ± 1.0 (10×10), and 20.8 ± 1.9 (15×15), to give an idea about the statistical errors in the saturated width.

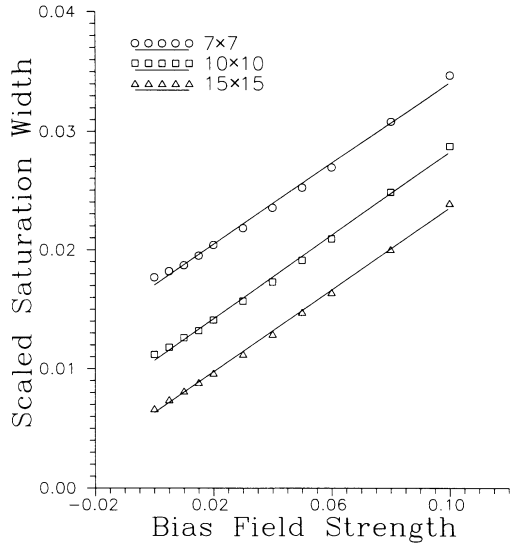

FIG. 7. Scaled saturated width ($W_s/L^{2\alpha}$) vs the bias field strength B_x for different sample sizes L.

and f is some function of the bias field strength. We find that $\alpha=1.25\pm0.10$. f seems to scale with the bias field B_x with a slope $m=0.170\pm0.004$, as we see from Fig. 7, where (W_s/A^{α}) is plotted against B_x. The scaling behavior is rather good considering the limitations on the sample sizes and fluctuations in the data. These simulations took about 1200 hours of CPU on RISC machines.

In summary, in our three dimensional fluid-flow model, we observe a diffusive behavior for the front in short time, followed by a nonuniversal power-law behavior for the front propagation at low values of the driven fields. The interface width saturates in the asymptotic regime. The saturated width scales with the cross-sectional area of the system with an exponent $\alpha=1.25$, and with the bias field strength with an exponent $m=0.17$. Thus, with our idealized model for the spreading of the fluid from a source (a planar river front), we are able to predict how fast the wet front moves into the dry (unsaturated) land: a slow (diffusive) propagation is followed by a faster invasion which depends on the pressure gradient (i.e., the bias). This study also shows that the spread in the frontal wetland area (interface width) will eventually attain a constant value (saturated width) which depends on the size of the source.

Computer simulations were performed on a SGI RISC-3000 computer at the Mississippi Center for Supercomputing Research, and IBM RISC-6000 (550 and 320) at USM's Center for Academic Computing and Program in Scientific Computing. Financial support from a NSF-EPSCoR grant is also acknowledged.

[1] S. F. Edwards and D. R. Wilkinson, Proc. R. Soc. London Ser. A **381**, 17 (1982).
[2] M. Kardar, G. Parisi, and Y.-C. Zhang, Phys. Rev. Lett. **56**, 889 (1986).
[3] D. Stauffer and J. G. Zabolitzky, Phys. Rev. Lett. **57**, 1809 (1986); D. E. Wolf and J. Kertesz, Europhys. Lett. **4**, 651 (1987); P. Devillard and H. E. Stanley, Physica A **160**, 298 (1989).
[4] F. Family, Physica A **168**, 561 (1990); P. Meakin, P. Ramanlal, L. M. Sander, and R. C. Ball, Phys. Rev. A **34**, 5091 (1986); D. Liu and M. Plischke, Phys. Rev. B **38**, 4781 (1988); J. M. Kim and J. M. Kosterlitz, Phys. Rev. Lett. **62**, 2289 (1989).
[5] *Dynamics of Fractal Surfaces,* edited by F. Family and T. Vicsek (World Scientific, Singapore, 1991).
[6] J. Krug and H. Spohn, Phys. Rev. Lett. **64**, 2332 (1990).
[7] Z.-W. Lai and S. Das Sarma, Phys. Rev. Lett. **66**, 3195 (1991).
[8] T. Natterman, S. Stepanow, L.-H. Tang, and H. Leschhorn, J. Phys. II (France) **2**, 1483 (1992); L.-H. Tang and H. Leschhorn, Phys. Rev. A **45**, R8309 (1992).
[9] A. Karma and C. Misbah, Phys. Rev. Lett. **71**, 3810 (1993).
[10] J. Koplik and H. Levine, Phys. Rev. B **32**, 280 (1985).
[11] N. Martys, M. O. Robbins, and M. Cieplak, Phys. Rev. B **44**, 12 294 (1991).
[12] E. Willett and R. B. Pandey, Phys. Rev. Lett. **65**, 3413 (1990).
[13] F. Family and R. B. Pandey, J. Phys. A **25**, L745 (1992).
[14] R. Bidaux and R. B. Pandey, Phys. Rev. E **48**, 2382 (1993).
[15] S. V. Buldyrev, A.-L. Barabasi, C. Caserta, S. Havlin, H. E. Stanley, and T. Vicsek, Phys. Rev. A **45**, R8313 (1992);

A.-L. Barabasi, M. Araujo, and H. E. Stanley, Phys. Rev. Lett. **68**, 3729 (1992).

[16] M. A. Rubio, C. A. Edwards, A. Dougherty, and J. P. Gollub, Phys. Rev. Lett. **63**, 1685 (1989).

[17] R. T. Tung and F. Schrey, Phys. Rev. Lett. **63**, 1277 (1989).

[18] *Random Fluctuations and Pattern Growth,* edited by H. E. Stanley and N. Ostrowsky (Kluwer Academic, Dordrecht, 1988).

[19] M. Sahimi, Rev. Mod. Phys. **65**, 1393 (1993).

[20] J. A. Pojman, R. Craven, A. Khan, and W. West, Phys. Chem. **96**, 7466 (1992).

[21] *Microscopic Simulations of Complex Hydrodynamic Phenomena,* edited by M. Mareschal and B. L. Holian (Plenum, New York, 1992); *Proceedings of the NATO Advance Research Workshop on Lattice Gas Methods for PDE's: Theory, Application and Hardware,* edited by G. Doolen [Physica D **47** (1991)].

[22] E. Salomons and M. Mareschal, Phys. Rev. Lett. **69**, 269 (1992).

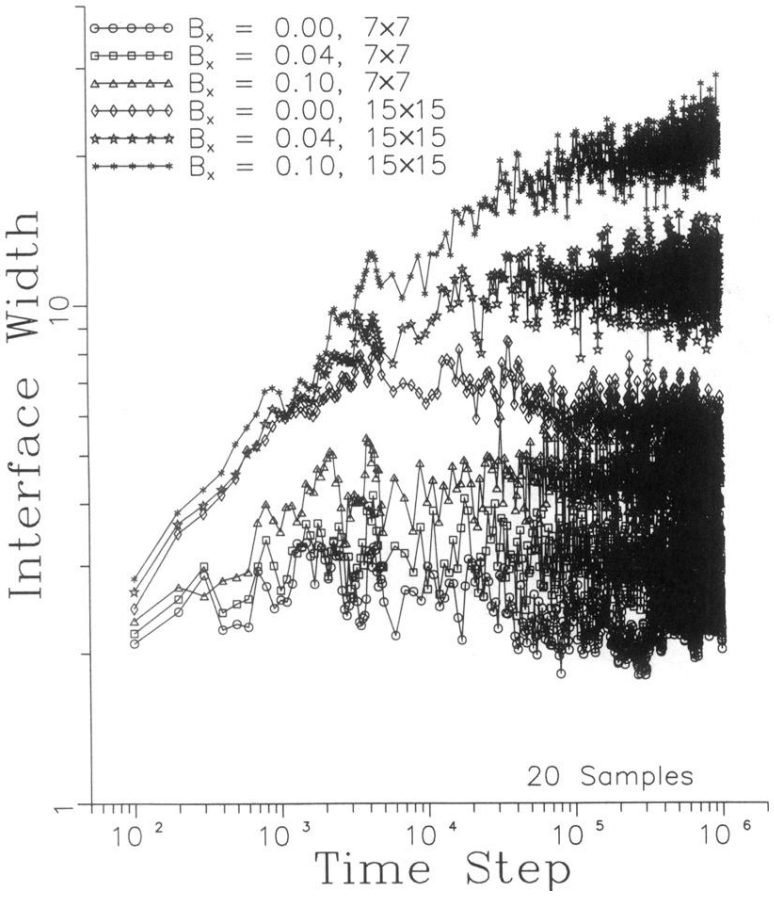

FIG. 5. Interface width vs time step on a log-log scale for various values of B_x with samples $7\times7\times L_x$ and $15\times15\times L_x$; $L_x = 100\,000$.